

The silicon matrix for the prototype of the Dark Matter Particle Explorer

R.R.Fan, F.Zhang, W.X.Peng, Y.F.Dong, K.Gong, S.Yang, D.Y.Guo,
J.Z.Wang, M.Gao, X.H.Liang, J.Y.Zhang, X.Z.Cui, Y.Q.Liu, H.Y.Wang

Institute of High Energy Physics Chinese Academy of Sciences, Beijing P.R.China

Abstract

A new generation detector for the high energy cosmic ray - the DAMPE(DARK Matter Particle Explorer) is a satellite based project. Its main object is the energy measurement of the cosmic ray nuclei from 100GeV to 100TeV, the high energy electrons and gamma ray from 5GeV to 10TeV. A silicon matrix detector described in this paper, is employed for the sea level cosmic ray energy and position detection while the prototype testing of the DAMPE. It is composed by the 180 silicon PIN detectors, which covers an area of $32 * 20cm^2$. The primary test result shows a good MIPs discrimination.

Keywords: Dark matter, silicon matrix, cosmic ray

1. Introduction

2 With the results of AMS-02[1], ATIC[2], PAMELA[3] and FERMI[4],
3 more and more proofs pointed the electron excess of cosmic electrons. With
4 a requirement of higher and more precise energy measurement, a dark matter
5 search satellite project DAMPE has been put forward.

6 The main scientific objective of DAMPE is to measure electrons and
7 photons with much higher energy resolution and energy reach than achievable
8 with existing space experiments in order to identify possible Dark Matter
9 signatures. It has also great potential in advancing the understanding of the
10 origin and propagation mechanism of high energy cosmic rays, as well as in
11 new discoveries in high energy gamma astronomy.

12 There are four sub-detector in the DAMPE system, the plastic scintil-
13 lator(PSD), the silicon tracker(STK), the BGO electromagnetic calorime-
14 ter(BGO) and the neutron detector.(see Figure 1)

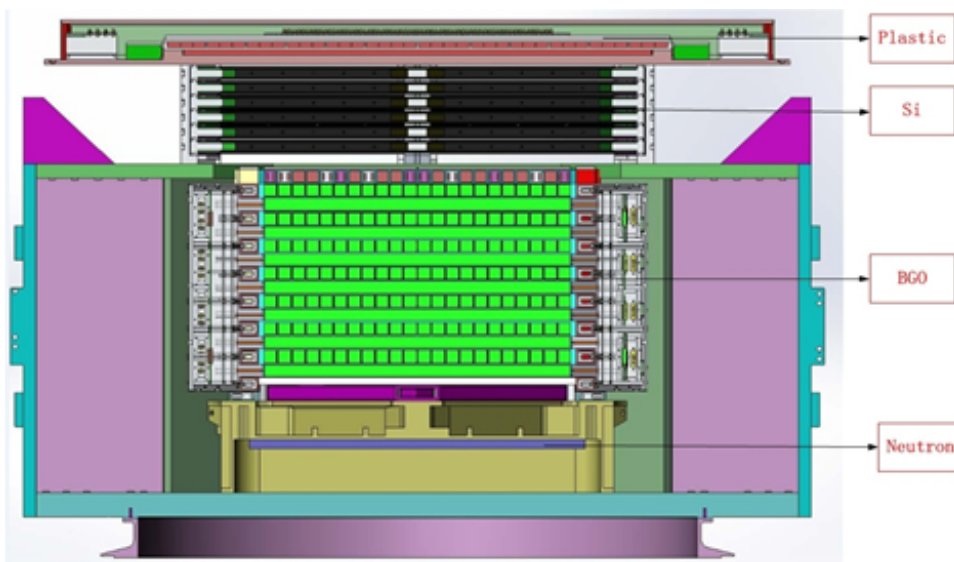


Figure 1: The schematic of DAMPE detector: The components of the DAMPE are PSD, STK, BGO and the neutron detector from top to bottom.

15 The plastic scintillator and silicon tracker are employed to charge parti-
 16 cles' discrimination and reconstruction the track. The silicon tracker with
 17 tungsten converters can also distinguish the gamma ray and electrons. The
 18 STK is followed by an imaging calorimeter of about 31 radiation lengths
 19 thickness, made up of 14 layers of BGO bars in a hodoscopic arrangement.
 20 A layer of neutron detectors is added to the bottom of the calorimeter for the
 21 proton/electron discrimination. The total thickness of the BGO calorimeter
 22 and the STK correspond to about 33 radiation lengths, making it the deepest
 23 calorimeter ever used in space.

24 For electrons and photons, the detection range of the DAMPE is 5 GeV -
 25 10 TeV, with an energy resolution of about 1% at 800 GeV. For cosmic rays,
 26 the detection range is 100 GeV - 100 TeV, with an energy resolution better
 27 than 40% at 800 GeV. The geometrical factor is about $0.3m^2sr$ for electrons
 28 and photons, and about $0.2m^2sr$ for cosmic rays. The angular resolution is
 29 0.1° at 100 GeV.

30 During the DAMPE prototype testing, a silicon matrix built by the Insti-
 31 tute of High Energy Physics(IHEP), the Chinese Academy of Sciences(CAS),
 32 serves as the silicon tracker. Followed chapters describe the details of the
 33 silicon matrix construction and test.

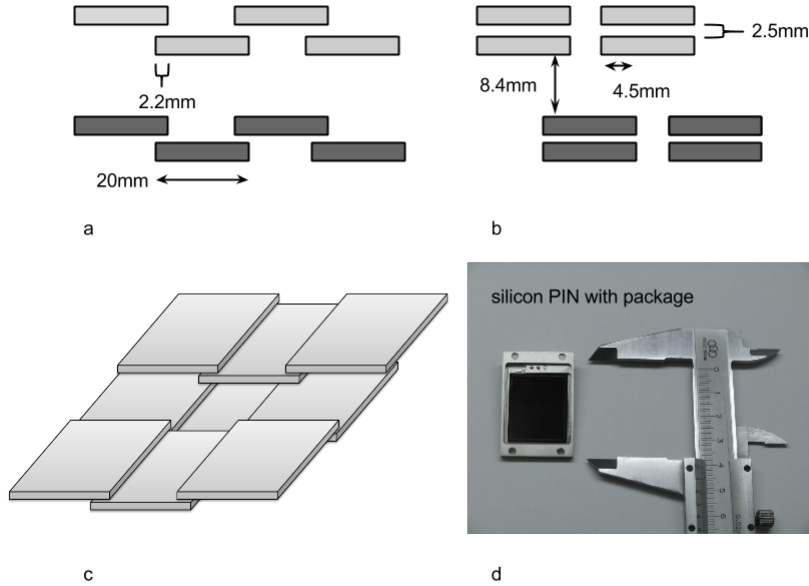


Figure 2: Illustrations of the matrix structure: a,b,c are different axes view of the silicon matrix. d is the photo of the silicon PIN detector with package.

34 2. The detector structure

35 2.1. the silicon matrix

36 In accordance of the required sensitive area, the matrix is composed of 180
 37 large area silicon PIN detectors(see Figure 2 d). Each of them has an active
 38 area of $20 * 25mm^2$ and 0.5mm thickness. The full depletion voltage for the
 39 selected detectors is 40 V, while the operation voltage is 60 V. The measure
 40 leak current of detectors is under 100 nA. The detector after selection is
 41 attached on a ceramic chip in a Kovar package.

42 To achieve a better detection efficiency of incident particles over $\pm 60^\circ$,
 43 every detector has a small overlap to the neighbor ones.(see Figure 2 c) The
 44 overlap is determined by the calculation and confirmed by the fast simulation.

45 While the assembling, the detector is fixed on the readout PCB and an
 46 aluminum frame via four screws. The detectors on top and on bottom are
 47 combined in two layers respectively. Figure 3 shows the photograph of the

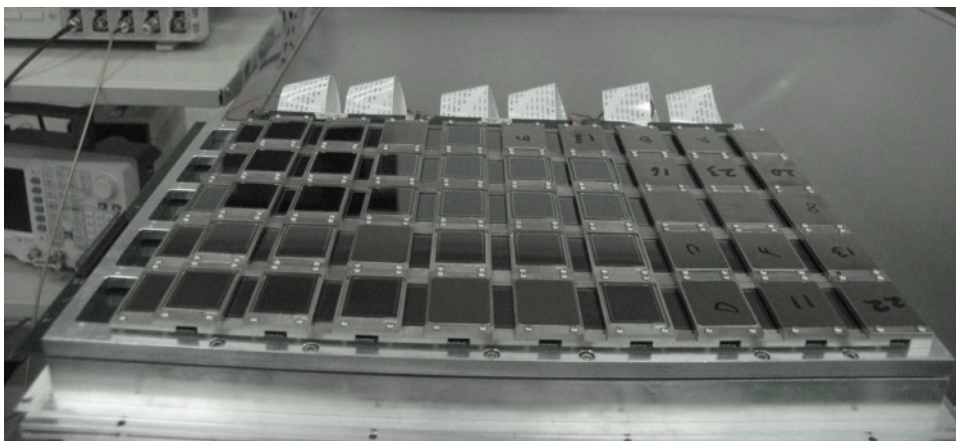


Figure 3: The photo of the top layer of the matrix: the 90(18*5) silicon PINs on top of the matrix, which is above the bottom layers.

48 top layer matrix. As this structure, the silicon matrix can achieved an active
49 area up to $32 * 20cm^2$.

50 *2.2. the electronics*

51 As shown in Figure 4, the readout electronics system of the matrix consists
52 an ASIC PCB and a control PCB. A aluminum box is employed to shield the
53 detectors and the front-end electronics(FEE) from the surrounding light and
54 the electro-magnetic interference. A VA140 readout PCB is mounted on the
55 back of each layer. The signals through the flex are read out by six VA140
56 chips, which are controlled by an FPGA. The DAQ communicated with the
57 computer via the USB bus.

58 The VA140 is a 64-channel, low noise and high dynamic range charge
59 measurement ASIC designed by IDEADS (Norway)[5]. It is an updated
60 version of the VA64HDR9A ASIC, which is used by AMS[6], implemented in
61 0.35um process for lower power consumption and better radiation tolerance.
62 Each channel contains a charge sensitive preamplifier, a shaper circuit and
63 a sample-hold circuit. Since the primary package can only afford 32 pins
64 output, we used the half of all the 64 channels to readout signals in every
65 VA140.

66 The control board is used for the VA140 control, the analog signal dig-
67 italization and the data communication. It contains a power module (the
68 HV and the regulator), a controlling FPGA(XC3S500E), a 14-bit 3MSPS
69 ADC(AD9243) and a USB interface chip(CY7C68013). A level shift circuit

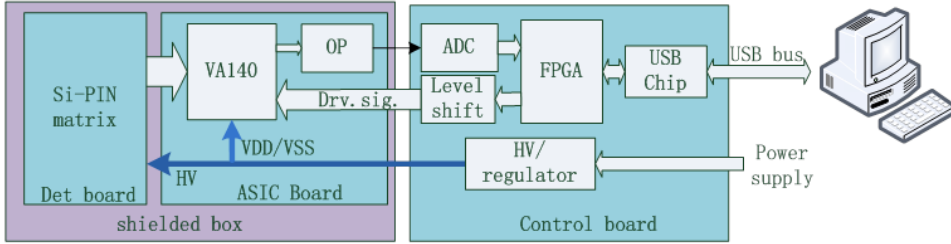


Figure 4: The readout schematic of the matrix: the matrix and the FEE(ASIC board) are placed in a shield box, the control board transfer the data to PC via USB bus.

70 from $0 \sim 3.3V$ to $-2V \sim +1.5V$ is used in the control board, due to the
 71 mismatched level voltage between the FPGA and the VA140.

72 The DAQ is based on a LabWindows GUI online software, while the
 73 offline data analysis is undertaken with the ROOT framework. In the test of
 74 electronics, An 100Hz random trigger is induced in to acquire the pedestals
 75 of every channel. We get an average noise of the channels is about 0.35 fC.

76 3. The cosmic ray test

77 There are two requirements of this matrix, giving the particle charge in-
 78 formation and the track reconstruction. The test in laboratory is completed
 79 with the sea level cosmic ray. In this test, we can get the unit charge re-
 80 sponse(MIPs) and an approximately position distribution.

81 A simple telescope system is set up for the test, which can be seen in
 82 Figure 5. The grey box labeled 1,2,3 stand for plastic scintillators. The area
 83 of scintillator 1 and 3 is $40 * 40cm^2$, which covers the whole surface of the
 84 matrix. The silicon matrix is placed in the middle of the plastic scintillators.
 85 When the incident particle pass through, this two plastic scintillators give
 86 the coincidence trigger to the DAQ. With a long time test, the MIPs energy
 87 spectrum can be obtained in readout channels. To get a position sensitive
 88 plot, a smaller scintillator 2 with a area of $12 * 10cm^2$ is inserted into the
 89 scintillator 1 and 3 as the indicator.

90 After 10 hours cumulating, the spectrum of each channel is obvious. Be-
 91 cause of the angle's effect, the charge resolution can't be directly derived
 92 from these spectrums. We still get clear views of the MIPs' peak in 175
 93 channels(97%). Figure 6 shows the first 4 channels' cumulate spectrums.

94 In the position sensitive testing, we got the MIPs counts map both of
 95 the top and the bottom layer(see Figure 7). In the plot, the X and Y axis

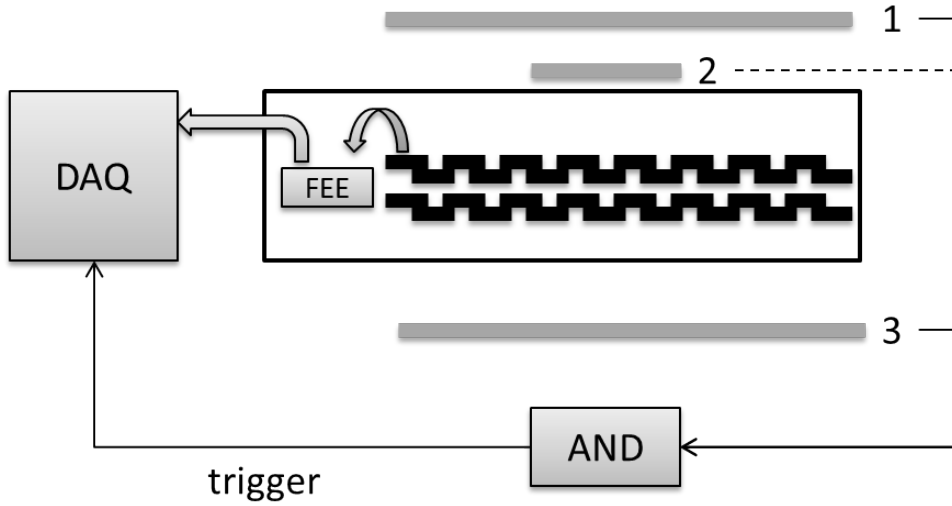


Figure 5: The telescope system of the cosmic ray test: the 1,2,3 stand for three scintillators, which give the trigger to the DAQ. The matrix is in the middle of these scintillators.

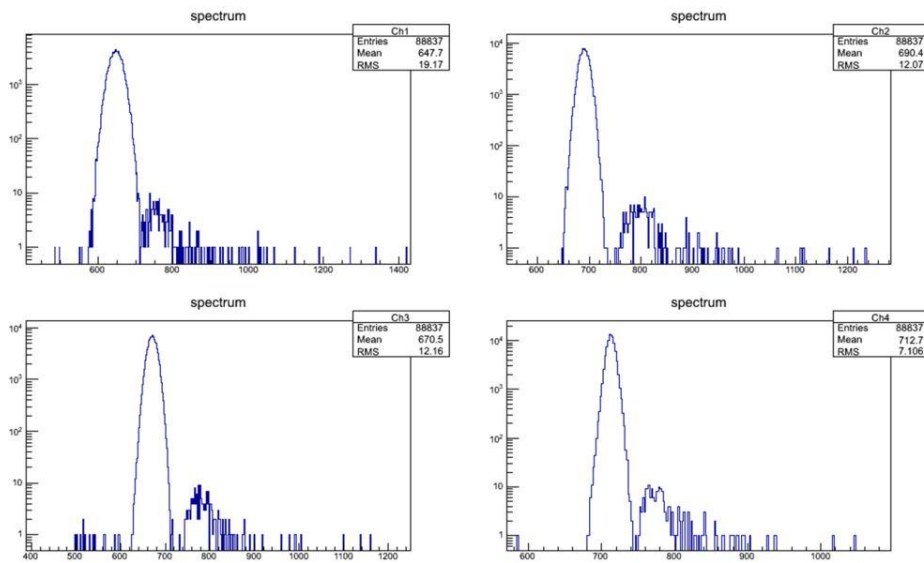


Figure 6: The spectrums of MIPs in the first four channels: the X axis is ADC number, the Y is counts.

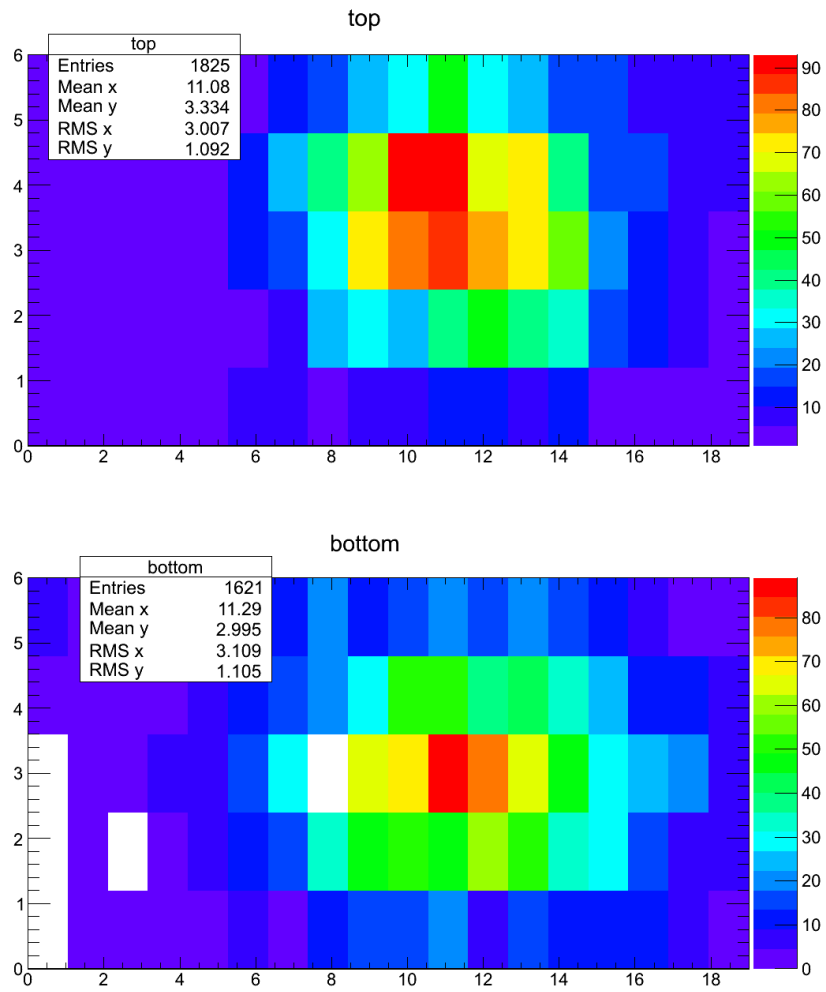


Figure 7: The lego plot of the position sensitive test: the X and Y axis unit is the detector channel. The palette gives the counts of MIPs

96 unit is the readout channel. The color shows different counts of the MIPs in
97 each detector. In the figure, we can see that except 5 bad channels in the
98 bottom layer(the white pixels), the gravity of two layers is almost same in
99 X axis. An offset about half of Y unit exists in the Y axis, because of the
100 detector structure(see Figure 2). The spot covers an area about 5*3, which
101 is in accord with the small-sized scintillator.

102 **4. Conclusion**

103 With the cosmic ray test, the matrix can distinguish the MIPs signal
104 from the electronics noise clearly, while the position can be confirmed by the
105 channel sequence. Through a long time running, the matrix is optimized for
106 the DAMPE prototype. The results of the DAMPE prototype test will be
107 presented in near future.

108 **5. Acknowledgements**

109 This work is supported by the Chinese Strategic Priority Research Pro-
110 gram in Space Science, CAS. The authors also greatly appreciated the col-
111 laboration with the DAMPE colleagues from the University of Science and
112 Technology of China(USTC) and the Purple Mountain Observatory(PMO)
113 during the electronics and the DAMPE prototype test.

114 **References**

- 115 [1] M. Aguilar et al., Phys. Rev. Lett. 110, 141102(2013)
- 116 [2] J. Chang, J. H. Adams, H. S. Ahn et al, Nature 456, 362-365 (2008)
- 117 [3] O. Adrianiet al., Nature 458, 607 (2009)
- 118 [4] M. Ackermann et al., Phys. Rev. Lett. 108, 011103(2012)
- 119 [5] VA140 documentation - V0R1
- 120 [6] G. Ambrosi, Nuclear Instruments and Methods in Physics Research A
121 435 (1999) 215-223